In-orbit vibration testing of spacecraft structures

F. Poncelet, G. Kerschen, JC. Golinval
University of Liège, Aerospace and Mechanical Engineering Department,
Chemin des Chevreuils 1, B-4000, Liège, Belgium
e-mail: **fponcelet@ulg.ac.be**

Abstract

In-orbit modal testing can be an interesting tool for the monitoring of spacecraft structures. In these applications, it is impossible to measure or to control the excitation resulting, for instance, from an impact with a small asteroid or from the working engines. Consequently the only realistic methodology must be an output-only modal analysis, also called Operational Modal Analysis (OMA). This paper proposes another way of doing OMA where the post-processing (i.e. the physical modal parameter extraction) is simplified and automated. The methodology uses the Blind Source Separation (BSS) techniques which attempt to recover the source signals only from their observed mixtures. In case of structural dynamic responses, the source signals and the mixing matrix are equivalent to the modal coordinates and the mode matrix, respectively. The paper describes the complete methodology including the post-processing, and its feasibility is demonstrated using a numerical application modeling a truss satellite with the FE method.

1 Introduction

The accurate knowledge of the dynamics characteristics is essential for the design, validation and even for the monitoring of many engineering structures. Numerous approaches were developed experimentally to estimate the modal parameters. The so-called Experimental Modal Analysis (EMA) methodologies require the knowledge of the dynamic response as well as of the applied excitation (input-output techniques). But in many applications (for instance for structures in their working environment), the actual loading conditions cannot be measured and output-only measurements are available. This is especially the case in civil engineering applications or for satellite and spacecraft structures, where an interaction with the structure is not conceivable.

Consequently, the used methodology must be an output-only modal analysis, also called Operational Modal Analysis (OMA). Several OMA methodologies have been developed the last decades. For example, two well-known and well-established methods are the Ibrahim [1] method and the Stochastic Subspace Identification method (and all its variants) [2].

The last few years, signal processing techniques have been used to perform OMA through the estimation of the modal coordinates. For instance, Lardies et al. [3] exploit the wavelet transform to determine the response of each mode and, subsequently, to compute the modal parameters. In [4], output-only data are processed using the empirical mode decomposition (also known as Hilbert-Huang transform) to identify the different modal contributions. Digital band-pass filters are considered by Kim et al. [5] for the same purpose. Although attractive in principle, these signal processing-based methods present several drawbacks such as edge effects and difficulty in identifying closely spaced modes.

In this paper, we propose to apply the Blind Source Separation (BSS) techniques in order to decompose the measured responses into the modal coordinates. Indeed, using the concept of virtual sources, a one-to-one relationship between the vibration modes and the BSS modes (i.e.. the mixing matrix) was demonstrated [6], allowing the use of BSS for modal analysis. Since then, different BSS algorithms were tested, and one of them (namely the Second-Order Blind Identification, SOBI) seemed to perform quite well [7, 8].

This technique is applied herein to a numerical system, representing a truss satellite, which contains very closed eigenfrequencies. The dynamic response is obtained using a finite element model. The aim of the paper is then to prove the usefulness of the methodology for such a kind of problem and also for large number of sensors. The modal analysis is also performed using the stochastic subspace identification, for a comparison.

2 Blind source separation and modal analysis

2.1 Theoretical background

Blind Source Separation (BSS) techniques were initially developed for signal processing in the early 80's, but during the last decade the number of the application fields never stopped increasing.

The main ambition of BSS is to recover the unobservable inputs of a system, called the sources s_i, only from the measured outputs x_i even though very little, if anything, is known about the mixing system. The simplest BSS model assumes the existence of n sources signals $s_1(t), ..., s_n(t)$ and the observation of as many mixtures $x_1(t), ..., x_n(t)$. Note that the focus is set on systems with linear and static mixtures. Using matrix notations the noisy model can be expressed as

$$\mathbf{x}(t) = \mathbf{A} \cdot \mathbf{s}(t) + \boldsymbol{\sigma}(t) \tag{1}$$

where $\boldsymbol{A}$ is referred to as the mixing matrix, and $\boldsymbol{\sigma}$ is the noise vector corrupting the data.

Most BSS approaches are based on a model in which the sources are independent and identically distributed variables. The objective of SOBI is to take advantage, whenever possible, of the temporal structure of the sources to facilitate their separation. The SOBI algorithm consists in jointly diagonalizing several covariance matrices. The complete explanation of the underlying theory is beyond the aim of this paper but for further details about the SOBI method, the interested reader can refer to [9, 7].

2.2 From signal processing to modal analysis

2.2.1 Concept of virtual source

The dynamic response of mechanical systems that are considered in the present study is described by the equation

$$\mathbf{M} \cdot \ddot{\mathbf{x}}(t) + \mathbf{C} \cdot \dot{\mathbf{x}}(t) + \mathbf{K} \cdot \mathbf{x}(t) = \mathbf{f}(t) \tag{2}$$

where $\mathbf{M}$, $\mathbf{C}$ and $\mathbf{K}$ are the mass, damping and stiffness matrices, respectively. The vector $\mathbf{f}$ represents the real excitation sources applied to the structure. The system response $\mathbf{x}(t)$ may be expressed as a mixture of these **real sources** $\mathbf{f}(t)$. Unfortunately, this mixture is a convolutive product between the impulse response function, denoted $\mathbf{h}(t)$, and the sources $\mathbf{f}(t)$, and the separation of convolutive mixtures of sources is not yet completely solved.

An interesting alternative is to use the modal expansion. Indeed, the m normal modes $\mathbf{n}_{(i)}$ form a complete basis for the expansion of any m-dimensional vector (if m is the number of degrees of freedom). Then the response can be expressed using modal superposition

$$\mathbf{x}(t) = \sum_{i=1}^{m} \mathbf{n}_{(i)} \cdot \eta_i(t) = \mathbf{N} \cdot \boldsymbol{\eta}(t) \tag{3}$$

where the weight coefficients η_i are in fact the modal coordinates and represent the amplitude modulation of the corresponding normal modes $\mathbf{n}_{(i)}$. The similarity between equations (1) and (3) shows that the modal coordinates may act as **virtual sources** (which are statistically independent as proved in [6, 7]) regardless of the number and type of physical excitation forces. In addition, the time response can be interpreted as a static mixture of these virtual sources, which renders the application of the BSS techniques possible.

The SOBI algorithm (which requires sources with different spectral contents) is particulary appropriate for the separation of these sources. In the free response case of the system (2), the theoretical expression of the normal coordinates is an exponentially damped harmonic function

$$\eta_i(t) = Y \cdot exp(-\xi_i \cdot \omega_i \cdot t) \cdot cos(\sqrt{1-\xi_i^2} \cdot \omega_i \cdot t + \alpha_i) \tag{4}$$

where ω_i and ξ_i are the natural frequency and damping ratio of the i^{th} mode, respectively. The amplitude Y and the phase α are constants depending on the initial conditions. The modal coordinates are then monochromatic, with different spectral contents.

2.2.2 Procedure details

In summary, a simple modal analysis procedure is proposed, using the modal coordinates as virtual sources. The procedure includes the following steps:

1. Perform experimental measurements of the structure response to obtain time series at different sensing position.
2. Apply SOBI directly to the measured time series to estimate the mixing matrix $\mathbf{A}$ and the sources $\mathbf{s}(t)$.
3. The mode shape matrix simply corresponds to the mixing matrix $\mathbf{A}$.
4. In the case of random excitation, the identified sources are transformed into free decaying responses using NExT (Natural Excitation Technique) algorithm [10].
5. The identification of the other modal parameters (frequencies and damping ratios) is carried out by fitting the time series of the sources $\mathbf{s}(t)$ with the theoretical expression (4).
6. The fitting error between the identified and fitted sources is then computed which allows to reject the non-reliable virtual sources easily.

3 Description of the case study

3.1 Modeling of the satellite

The considered structure is a large-scale truss satellite. The topology used for the modeling was inspired by the one presented in [11].

The central part is a six-meters length cylinder which is stiffened thanks to several internal shear panels. Two truss structures (made of tubular longerons, battens and diagonals) are symmetrically placed on both sides. The longerons are parallel to the axial direction (X-axis). The battens are the triangular structures which link the longerons together. The diagonals prevent the torsion mechanisms.

Shell elements are used to model the cylinder whereas beams (with tubular cross-section) make up the truss. All the dimensions and the properties used for the modeling are summarized in the table 1.

A satellite illustration is also presented in the figure 1.

Properties	
Total length	54 m
Young's modulus (E)	69000 Mpa
Poisson's ratio (ν)	0.33
Internal radius of longerons	37 mm
External radius of longerons	38 mm
Internal radius of diagonals and battens	12.5 mm
External radius of diagonals and battens	13 mm

Table 1: Material and geometrical properties of the truss

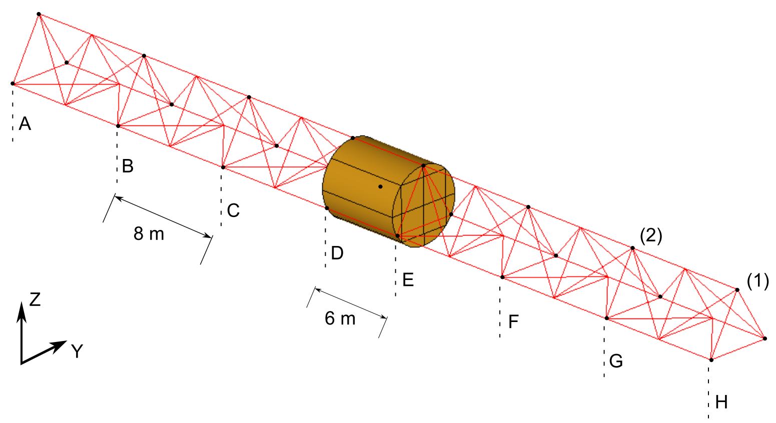

Figure 1: Geometry of the satellite
Three locations of measurements are defined for each vertical section A to H (black spots on the figure), and this along Y and Z
(1) and (2) are respectively the position of the initial non-zero condition (free response) and of the applied random force (random response)

Table 2: FEM eigenfrequencies and mode identification

Mode	1H	1V	1T	2T	2H	2V	3H	3V	4H	4V
Frequency (Hz)	6.55	6.56	7.69	7.78	9.39	9.39	12.20	12.21	12.45	12.46
Mode	5H	5V	6H	6V	3T	4T	7H	7V	8H	8V
Frequency (Hz)	16.93	16.94	17.04	17.04	20.93	20.95	22.65	22.65	22.67	22.68

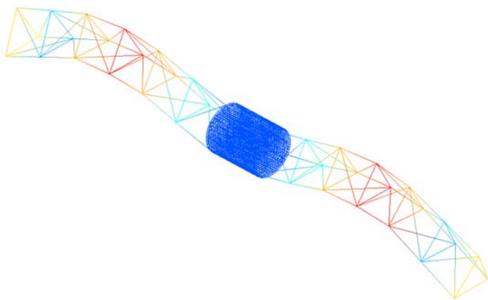

(a) Mode 7V - 22.65 Hz

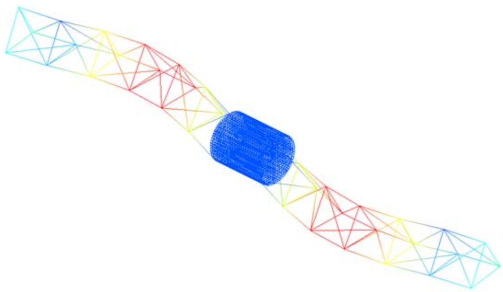

(b) Mode 6H - 17.04 Hz

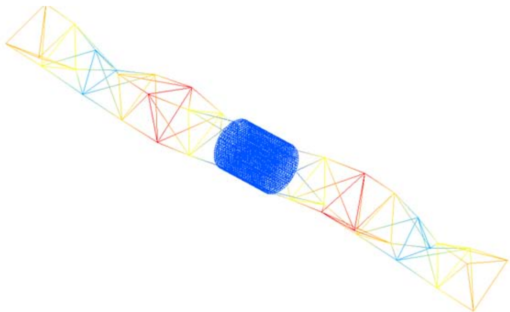

(c) Mode 3T - 20.93 Hz

Figure 2: Examples of mode shapes for the vertical, horizontal and torsion modes

3.2 FEM simulations

3.2.1 FE eigenmodes

In order to avoid the rigid body modes and also to prevent computational problems for the dynamic response, 18 (6 x 3) very soft ground-springs are added along the three principal directions (X, Y and Z) at the three vertices of the sections B and G (cf. figure 1).

Using the FE model mentioned above, the eigenmodes are easily computed. The focus is set on the frequency range $[0 - 23Hz]$ which corresponds to the 20 first (non rigid body) modes. The corresponding eigenfrequencies are very close to each others, as shown in table 2.

The twenty modes are divided into three parts regarding the mode shape:

- Modes 1V to 8V: bending in the vertical plane (XZ)
- Modes 1H to 8H: bending in the horizontal plane (XY)
- Modes 1T to 4T: torsion around the axial direction (X)

One mode shape from each group is depicted in figure 2.

Properties	
Modal damping	0.1%
Sampling frequency	153.6 Hz
Number of samples	18432
Simulation time	120 sec
Number of simulated sensors	48

Table 3: Properties used for the simulation of the dynamic responses

3.2.2 Dynamic response

The dynamic responses are computed using the modal superposition method, with the 60 first modes. The generic properties, which are used for all the simulations presented herein, are summarized in the table 3.

Twenty-four locations, corresponding to the three vertices of each sections A to H (cf. figure 1) are retained for the simulation along Y and Z. Thus 48 sensors are used for the modal analysis.

The simulations, and consequently the following studies, are divided in two parts:

The free response is computed using an non-zero initial velocity imposed at the upper part of the section H (vertex (1) in the figure 1).

The forced response is computed by applying a random (Gaussian) force at the upper part of the section G (vertex (2) in the figure 1). Note that in this case the random input is filtered around the frequency range of the computed FEM modes (used for the modal superposition) beforehand, e.g. [5-30 Hz].

4 Free response

The free response is first considered. This one is computed using a non-zero initial velocity condition which is applied vertically (along Z-axis) at one extremity of the truss, precisely at the vertex (1) (see the figure 1). The identification is then performed using the covariance-driven stochastic subspace identification (SSI) and then the SOBI algorithm.

In this section, only the vertical and torsion FEM modes are retained for comparison with the FEM modes. Indeed the horizontal modes are not as well excited, due to the vertical impact.

4.1 Subspace Identification Results

The SSI method is first used to extract the modal parameters. Because of the high number of closed eigenfrequencies contained in the response signal (more than 60 modes between 5 and 30 Hz), a high system order must be chosen. But because of time computation limitation, only the 6000 first samples are taken into account, which corresponds to the 40 first seconds.

The subspace identification is based on the computation of a stabilization diagram which allows the user to separate the actual eigenmodes and frequencies form the numerical ones. This phase requires as many problem resolutions as wished orders. The upper part of the stabilization diagram is presented in the figure 3(a). The diagram is very clear and after the manual mode selection, the Modal Assurance Criterium (MAC) matrix is computed to compare with the FEM modes (see figure 3(b)). This figure shows the very good correlation between SSI and FEM modes. The damping ratios (which were set to 0.1%) is also well correlated, as shown in figure 6(a).

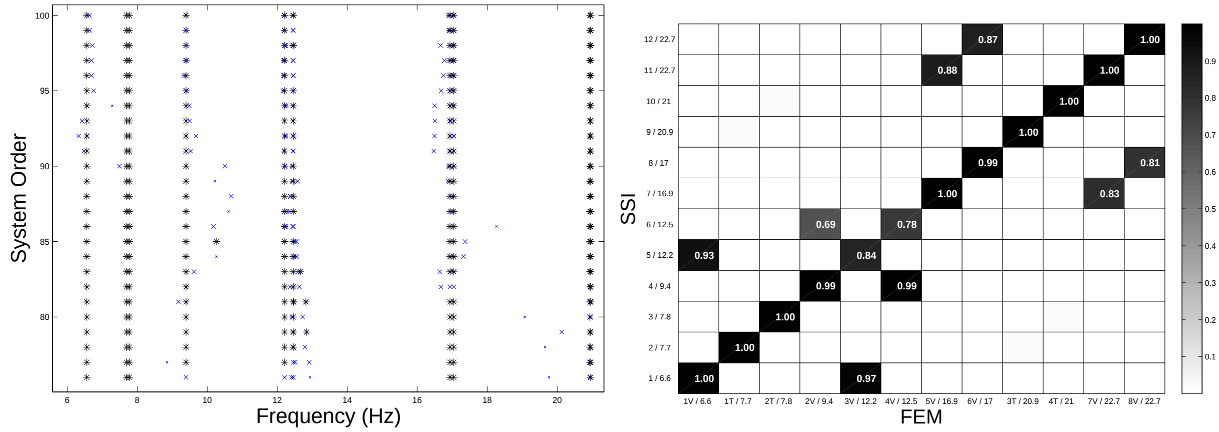

(a) Stabilization Diagram for SSI

(b) MAC matrix between SSI and FEM results

Figure 3: Stochastic Subspace Identification Results - Free response

4.2 SOBI Results

The same 6000 samples are now used to identify the modal parameters using the SOBI algorithm. Twenty delays ($N = 20$) are chosen for SOBI and they are defined in order to correspond to the frequencies belonging within the range of interest. In actual practice, if the sampling frequency ($f_{sampling}$) is correctly settled, it is easy to choose the delays as multiples of the time step: $\tau_i = i \cdot 1/f_{sampling}$ for $i = 1, ..., N$.

Even if the SOBI method is not based on a stabilization diagram, it is still necessary to separate the actual eigenmodes and frequencies from the non physical ones. Indeed, SOBI identify as many sources (or modes) as the sensors. The selection is an automatic process which is based on the fitting error computed for each source (through the theoretical modal coordinates formula, see section 2.2.1 and equation 4).

As mentioned above, 48 sources are identified. The fitting error is presented for each identified source in figure 4 with the corresponding MAC matrix. The mode selection is here based on the following criteria:

1. All the frequencies out of the **frequency range of interest** ([5-23Hz]) are rejected.
2. Only the fitting errors (red bars in the figure) **lower than 10%** are considered.
3. An interesting parameter (blue bars in the figure) is the participation factor which evaluate the importance of each source in the total response signal and could be interpreted as a **confidence factor**.

After the selection, the results are much more clear as seen in the figure 5. The corresponding identified damping ratios are also presented in figure 6(a). All the results are very satisfying if not as good as the SSI ones. Note however that the number of samples used for the identification could have been increased easily. Indeed the SOBI computation cost is lower than the SSI one and only one computation is performed since no stabilization diagram is necessary.

5 Forced response

In the forced response case study, a structural loading during all the acquisition time can be considered, which should improve the quality of the identification. For the signal considered herein, three different excitations are applied simultaneously at the location (2) (see figure 1): a vertical random force along Z-axis, an horizontal random force along Y-axis and finally a random torque around the X-axis. The three random loads are computed as explained in the section 3.2.2. This should excite all the 20 modes (the vertical and

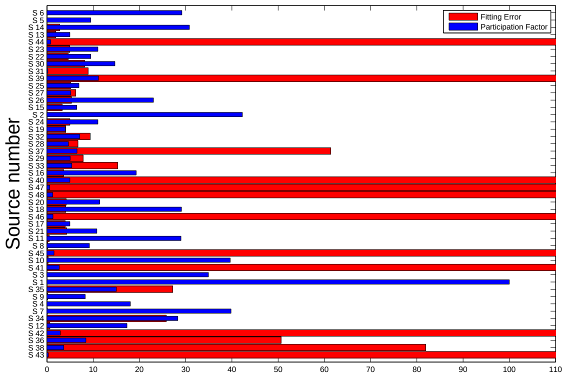

(a) Fitting Error (red) and Participation Factor (blue)

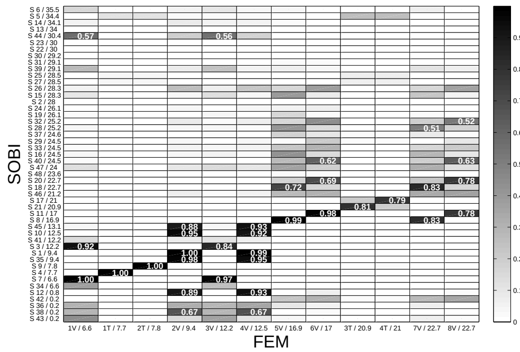

(b) MAC matrix between SOBI and FEM results

Figure 4: Untreated SOBI results - Free response

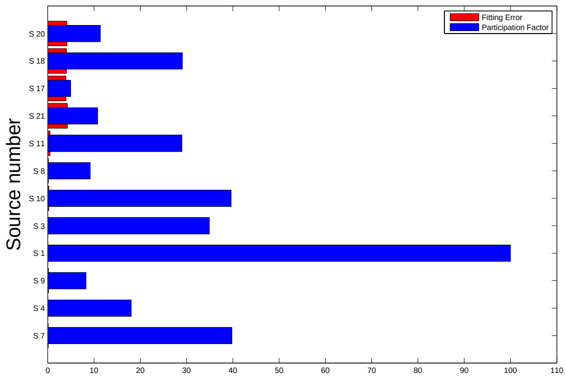

(a) Fitting Error (red) and Participation Factor (blue)

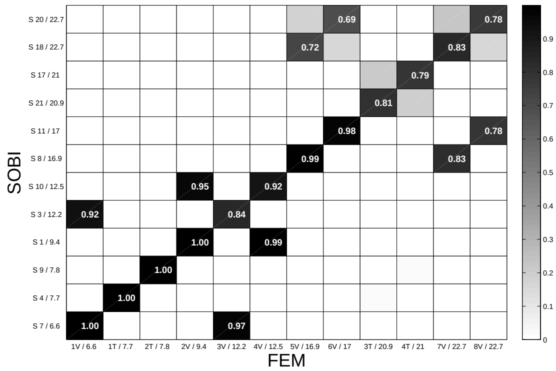

(b) MAC matrix between SOBI and FEM results

Figure 5: SOBI results after automatic selection - Free response

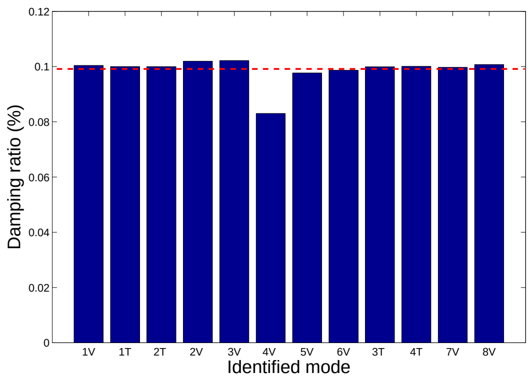

(a) Damping identified using SSI

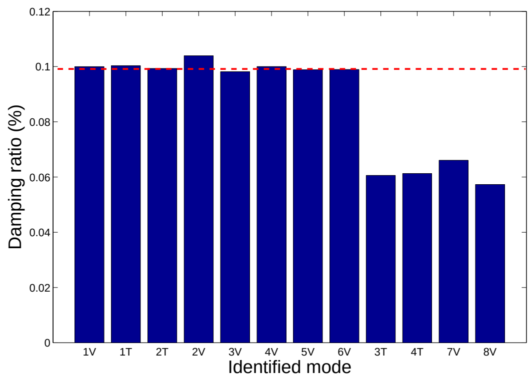

(b) Damping identified using SOBI

Figure 6: Value of the damping ratios (%) for both methods (expected value: 0.1%) - Free response

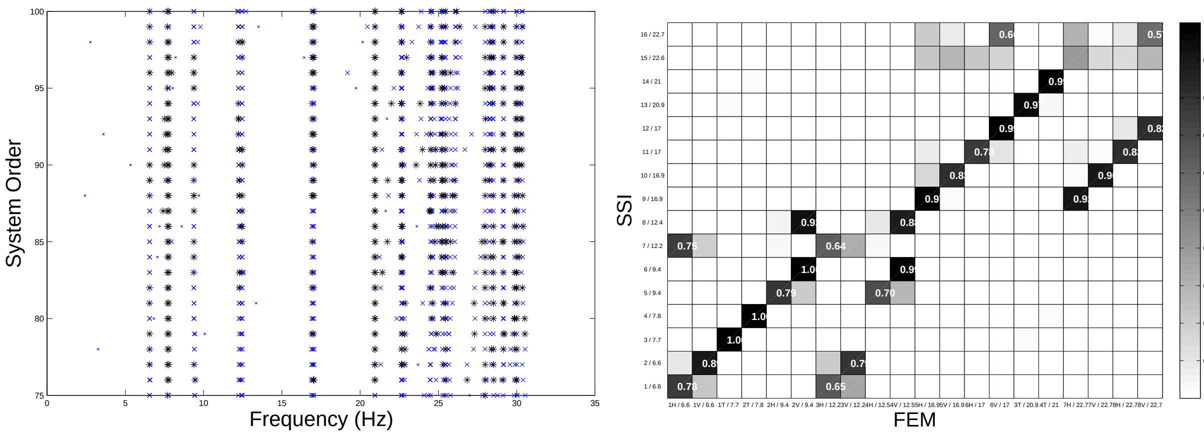

(a) Stabilization Diagram for SSI

(b) MAC matrix between SSI and FEM results

Figure 7: Stochastic Subspace Identification Results - Forced response

the horizontal bending ones as well as the torsion ones). In this section, all the 20 FEM modes belonging to the range [5-23Hz] are kept for the comparison.

The simulation generates a dynamic response for the first 120 seconds, using a sampling frequency still equals to 153.6 Hz. The 18000 first samples are used for the identification.

5.1 Subspace identification results

The identification is performed with the previous simulated signal from the order 50 to the order 100. The upper part of the stabilization diagram is presented in figure 7(a) which can be discussed as follows:

- All the eigenfrequencies in the frequency range [0-23Hz] are detected by the SSI method for almost all the computed orders (blue crosses $\times$).
- The damping stabilization is much more uncertain (black stars $*$) and this is also the case comparing the modes using MAC values between each order.
- Based on the only stabilization diagram, it seems to be difficult to determine one order that represent accurately the system and satisfy all the eigenfrequencies.

For this particular numerical test case, all the exact modes are perfectly known and so, even if delicate, the selection of the physical modes can be facilitated using the MAC matrix between the SSI results for each system order and the FEM results. This study is of course very tedious, the best MAC matrix is then selected and presented in the figure 7(b).

The subspace identification succeed in extracting correctly the majority of the twenty expected modes. 16 modes are accurately identified and only the modes 3V, 4H, 7V and 8H are not detected. For those 16 modes, the identified damping ratios (still set to 0.1% for all modes in the simulation) are presented in the figure 10(a). Because of the non stabilization, these ones are clearly less good than for the free response case study but are still very acceptable.

Note that some higher orders (over 100) have been studied and tested but the quality of the results did not increase.

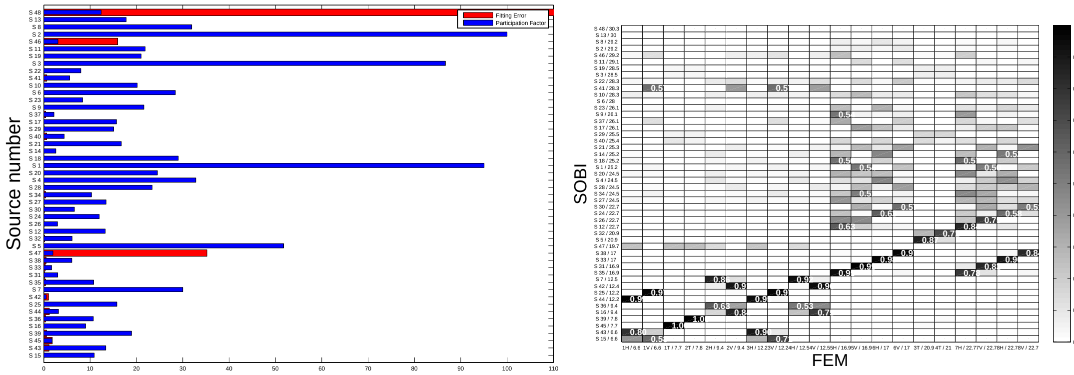

(a) Fitting Error (red) and Participation Factor (blue) (b) MAC matrix between SOBI and FEM results

Figure 8: Untreated SOBI results - Forced response

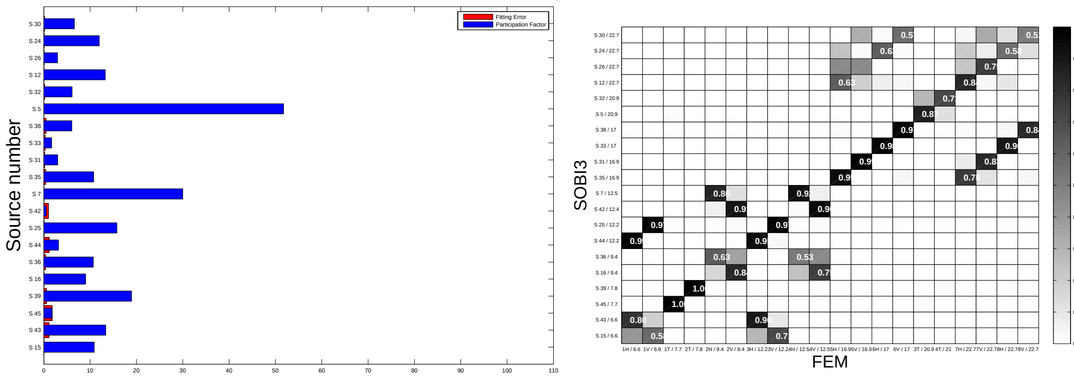

(a) Fitting Error (red) and Participation Factor (blue) (b) MAC matrix between SOBI and FEM results

Figure 9: SOBI results after automatic selection - Forced response

5.2 SOBI results

The same 18000-samples data set is considered for the SOBI identification. In this case, 40 delays are introduced as explained in the section 4.2. As for in the free response case 48 sources are separated (due to the 48 sensors). They are presented in the figure 8, as well as the corresponding fitting errors.

By definition the sources, which are identified for a random response, do not fit the theoretical formula 4. To use the automatic post-processing mode selection (as in the previous case), a free decaying response has to be computed for each source. This is performed using the Natural Excitation Technique (NExT) procedure. The interested reader may refer to [10] for further information.

After the mode selection which is performed using the same criteria as previously, 20 modes are kept. The corresponding MAC matrix is presented in the figure 9. Here again, the identification performs very well. It should be noted that the position of some modes are swapped over, but this is insignificant since the frequency gap is lower than 0.02 Hz. The damping ratios are presented in the figure 10(b).

6 Conclusions

In this paper, operational modal analyses are performed by extracting modal coordinates directly from structural responses through second-order blind identification. This technique, recently introduced in the literature, is applied to a numerical application for a free response as well as for a forced random response.

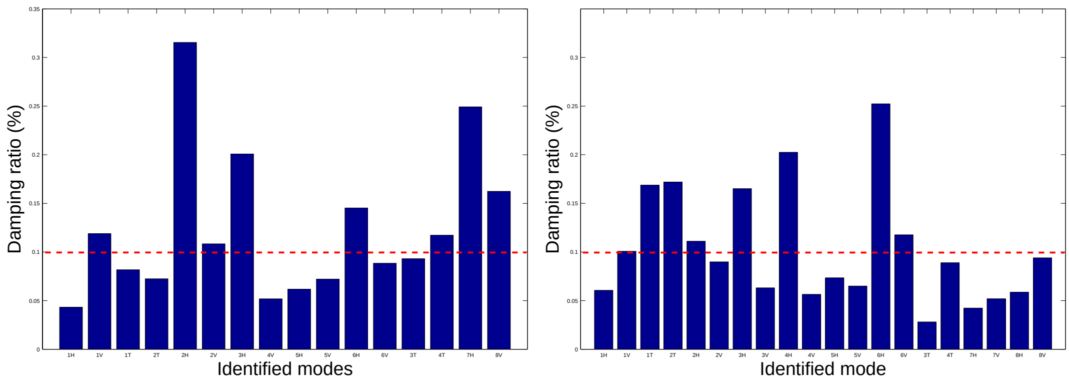

(a) Damping identified using SSI

(b) Damping identified using SOBI

Figure 10: Value of the damping ratios (%) for both methods (expected value: 0.1%) - Forced response

Numerous modes, close to each others, are excited: 20 modes between 6 and 23 Hz. The identification results show that the method holds promise for identification of mechanical systems:

- A truly simple identification scheme is proposed, because the straightforward application of SOBI to the measured data yields the modal parameters.
- A seemingly robust criterion has been developed for the selection of reliable sources which leads to an automatic post-processing. The use of stabilization charts, which always require a great deal of expertise and is time consuming for the user, is therefore avoided. In addition, the selection of a model order, a common issue for conventional modal analysis techniques such as SSI, is not necessary.
- Compared to SSI, the computation load is very reduced, which makes the method a potential candidate for online modal analysis.

A possible limitation of the method is that sensors should always be chosen in number greater or equal to the number of active modes.

Acknowledgements

The author F. Poncelet is supported by a grant from the Walloon Government (Contract N516108-VAMOSNL).

References

[1] S. Ibrahim and E. Mikulcik, “A time domain modal vibration test technique,” *Shock and Vibration Bulletin*, vol. 43, pp. 21–37, 1973.

[2] P. Van Overschee and B. De Moor, *Subspace Identification for Linear Systems: Theory, Implementation, Applications*. Kulwer Academic Publishers, 1996.

[3] J. Lardies, T. Minh Nghi, and M. Berthillier, “Modal parameter estimation using the wavelet transform,” *Archive of Applied Mechanics*, vol. 73, pp. 718–733, 2004.

[4] J. N. Yang, Y. Lei, S. L. Lin, and N. Huang, “Identification of natural frequencies and dampings of in situ tall buildings using ambient wind vibration data,” *Journal of Engineering Mechanics-Asce*, vol. 130, no. 5, pp. 570–577, 2004. 814FL Times Cited:4 Cited References Count:22.

[5] B. H. Kim, N. Stubbs, and T. Park, "A new method to extract modal parameters using output-only responses," *Journal of Sound and Vibration*, vol. 282, no. 1-2, pp. 215–230, 2005. 906SZ Times Cited:5 Cited References Count:19.

[6] G. Kerschen, F. Poncelet, and J. C. Golinval, "Physical interpretation of independent component analysis in structural dynamics," *Mechanical Systems and Signal Processing*, vol. 21, no. 4, pp. 1561–1575, 2007. 142KS Times Cited:1 Cited References Count:26.

[7] F. Poncelet, G. Kerschen, J. C. Golinval, and D. Verhelst, "Output-only modal analysis using blind source separation techniques," *Mechanical Systems and Signal Processing*, vol. 21, no. 6, pp. 2335–2358, 2007.

[8] S. I. McNeill and D. C. Zimmerman, "A framework for blind modal identification using joint approximate diagonalization," *Mechanical Systems and Signal Processing*, vol. In Press, Corrected Proof.

[9] A. Belouchrani, K. Abed-Meraim, J.-F. Cardoso, and E. Moulines, "A blind source separation technique using second order statistics," *IEEE Transactions on Signal Processing*, vol. 45, no. 2, 1997.

[10] I. James, G. H., T. G. Carne, and J. P. Lauffer, "The natural excitation technique (next) for modal parameter extraction from operating wind turbines," 1993. Other Information: PBD: Feb 1993 Other Information: PBD: Feb 1993 United States Other: ON: DE93010611 System Entry Date: 07/05/2005 Availability: OSTI; NTIS; GPO Dep. Source: SNL-A; SCA: 170602;990200; SN: 93000959378 Language: English.

[11] A. Salehian, E. M. Cliff, and D. J. Inman, "Continuum modeling of an innovative space-based radar antenna truss," *Journal of Aerospace Engineering*, vol. 19, no. 4, pp. 227–240, 2006.